01 Aug 1999

Slot and Aperture Coupling for Airflow Aperture Arrays in Shielding Enclosure Designs

Min Li

James L. Drewniak
Missouri University of Science and Technology, drewniak@mst.edu

Todd H. Hubing
Missouri University of Science and Technology

Richard E. DuBroff
Missouri University of Science and Technology, red@mst.edu

et. al. For a complete list of authors, see *https://scholarsmine.mst.edu/ele_comeng_facwork/1881*

Recommended Citation

Slot and Aperture Coupling for Airflow Aperture Arrays in Shielding Enclosure Designs

M. Li, J. L. Drewniak, T. H. Hubing, R. E. DuBroff, T. P. VanDoren

Electromagnetic Compatibility Laboratory
Department of Electrical Engineering
University of Missouri at Rolla
Rolla, MO 65409
mili@ece.umr.edu

Abstract: The coupling between apertures or slots in airflow arrays is investigated numerically by means of the method of moments (MoM). Application to shielding enclosure design is of particular interest. Justification for a previously extracted simple empirical design approach for the relation between the number N and size a of apertures, and the shielding effectiveness $\sim Na^3$ for an airflow aperture array is given. The coupling between slots is also investigated. The application limit of the empirical design approach is demonstrated.

I. Introduction

The integrity of shielding enclosures is compromised by slots and apertures for heat dissipation, CD-ROMs, I/O cable penetration, and plate-covered unused connector ports, among other possibilities. Radiation from slots can usually be minimized with gaskets, while it is more difficult to mitigate the radiation from apertures. With the utilization of high-frequency digital devices, perforation patterns with electrically small apertures instead of large openings in a shielding enclosure are employed for heat dissipation. Due to the total open area required for thermal purposes and mechanical reasons, there is a lower limit on the size of the apertures of the perforation pattern, which may result in EMI problems at high frequencies. Considerable work has been done on the energy coupling through one aperture [1], [2], and aperture arrays [3], while investigations of EMI as a function of the mutual coupling between apertures in an aperture array are limited. For example, an empirically determined relation for EMI from aperture arrays, $|E_{3m}| \sim Na^3$, where N is the number of apertures, and a the size of a single aperture, did not address a theoretical basis, or limitations for the N factor [4]. Previous work on the mutual admittance of multiple apertures concentrated on the mutual coupling of power, which was more suitable for near-field applications [5], [6], [7].

An electrically small aperture in one panel of a shielding enclosure, if not near the edge, can be treated approximately as a small hole in an infinite plane. Bethe's small hole theory models the electrically small aperture in an
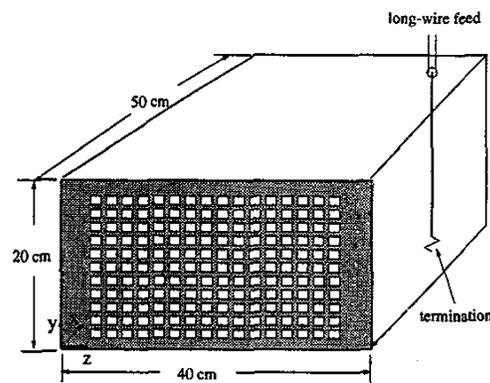

Figure 1. Configuration of the enclosure utilized for the perforation pattern study.

infinite plane with two perpendicular magnetic and electric dipoles [1]. The radiation from a single aperture is then calculated from the radiation of the dipoles. Aperture arrays are more complicated due to the mutual coupling between the apertures. The coupling between apertures and slots are investigated with MoM modeling herein. The results suggest that the radiated field is approximately proportional to the number of apertures even for the typically small aperture spacings in airflow aperture arrays used in practice, providing a justification for the empirical approach of $EMI \sim Na^3$ for square apertures. The mutual coupling between slots is more complicated, and is highly dependent on the slot orientation and spacing.

II. Experimental Results

EMI from an airflow aperture array with a large number of apertures was studied in a shielding enclosure mimicking an actual file server product. The geometry is shown in Figure 1. The enclosure was initially studied both experimentally and with FDTD modeling. The interior dimensions of the enclosure were $40\ cm \times 20\ cm \times 50\ cm$. One-inch copper tape with a conductive adhesive was used as an electromag-
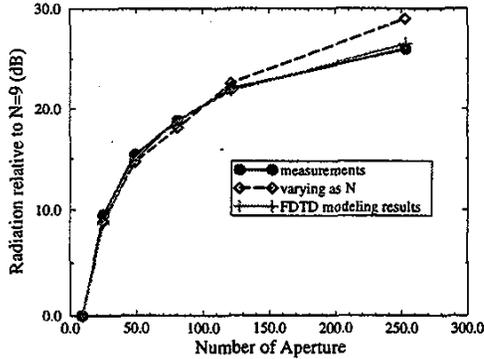
Figure 2. The EMI from an aperture array as a function of the number of apertures.

netic seal along the interior seams in the measurements. A terminated feed probe at $x = 43$ cm, $z = 33$ cm was employed as an excitation source. The center conductor of the probe was extended to span the width of the cavity with a 0.16 cm diameter wire, and terminated on the opposite cavity wall with a 1206 package size surface-mount (SMT) nominal 47 Ω resistor soldered to a 1.5″ × 1.5″ square of conductive adhesive copper tape. The enclosure was constructed of five pieces of 0.635 cm thick aluminum, and one plate of 0.165 cm thick aluminum. The 0.165 cm thick plate was used for the face containing a 252 1 cm × 1 cm (with a spacing of 0.5 cm) aperture array. Radiation from the enclosure was measured in a semianechoic chamber, employing a log-periodical antenna as the receiving antenna. A Wiltron 37247A Network Analyzer was used to measure the transmission coefficient $|S_{21}|$, which is related to the radiation.

The finite-difference time-domain (FDTD) method was employed to model the test enclosure. A cell size of 0.5 cm × 0.5 cm × 1.0 cm was used. Aluminum plates were modeled with perfect electric conducting (PEC) surfaces by setting the tangential electric field to zero on the cavity walls. The wire feed-probe was modeled using a thin-wire algorithm [8]. The source was modeled by a simple voltage source V_s, with a 50 Ω resistance incorporated into a single cell at the feed point. The resistor was modeled as a lumped element using a subcellular algorithm [9]. Perfectly-Matched-Layer (PML) absorbing boundary conditions were employed for the 3D FDTD modeling [10], and the PML absorbing layers were 8 cells away from the exterior of the shielding enclosure.

The measured and FDTD modeled EMI from the shielding enclosure as a function of varying aperture numbers is shown in Figure 2. The variation in the relative field level for different aperture numbers was nearly uniform in the frequency range from 0.3 GHz to 1.2 GHz. The number

of apertures was varied by masking a portion of the total aperture array ($N = 252$) footprint with copper tape. The aperture configurations tested always had the array located symmetrically about the center in the front panel. The results indicate that the radiation is directly proportional to the number of apertures N. The limit of application of the N factor, i. e., the effect of aperture mutual coupling, has not been investigated. The study reported herein investigated these aspects with MoM modeling.

III. MoM Formulation

The MoM was applied to obtain the field distributions inside the apertures, and the mutual coupling between apertures. The integral equation formulation for apertures in an infinite perfect electric conductor plane at $z = 0$ is [11]

$$[j\omega \vec{F}(\vec{r}) + \frac{j}{\omega\mu_0\epsilon_0} \nabla(\nabla \cdot \vec{F}(\vec{r}))] \times \hat{z} = \frac{1}{2}\vec{H}_-^{sc} \times \hat{z}, \quad (1)$$

where ω is the angular frequency, μ_0 is the free-space permeability, ϵ_0 is the free-space permittivity, $\vec{H}_-^{sc}$ is the short-circuited magnetic field for $z < 0$ (assuming there is no source at $z > 0$), and $\vec{F}(\vec{r})$ is the electric vector potential given by

$$\vec{F}(\vec{r}) = \frac{\epsilon}{4\pi} \int \int_A 2\vec{M}(\vec{r}') \frac{e^{-jk|\vec{r}-\vec{r}'|}}{|\vec{r}-\vec{r}'|} ds', \quad (2)$$

where k is the wave number, and $\vec{M}(\vec{r})$ is the equivalent magnetic current density in the aperture $\vec{M}(\vec{r}) = \vec{E}(\vec{r}) \times \hat{z}$ ($\vec{E}(\vec{r})$ is the electric field in the aperture). MoM using Rao's triangle basis functions was employed herein to obtain the magnetic current density $\vec{M}(\vec{r}')$ in the apertures [12]. The EMI at a distance of 3 m, assuming the far field (which is appropriate for the electric field at 3 m for $f > 500$ MHz), from the aperture arrays is calculated for a given $\vec{M}(\vec{r}')$ as

$$\vec{E}_{3m} \sim j\omega\vec{F}. \quad (3)$$

Assuming the footprint of the aperture array is much smaller as compared to the distance between the aperture array and the observation point R ($R = 3$ m for E_{3m}), E_{3m} is simplified as

$$\vec{E}_{at\ R} \simeq j\omega\frac{\epsilon}{4\pi}\frac{e^{-jkR}}{R} \int \int_A 2\vec{M}(\vec{r}')ds', \quad (4)$$

where $\int \int_A \vec{M}(\vec{r}')ds'$ is denoted as $\vec{M}_t$ for each aperture. The EMI is then directly related to $|\vec{M}_t|$, which is calculated from the MoM procedure.

IV. Aperture and Slot Coupling

Apertures were first investigated with the MoM modeling described above to quantify the mutual coupling in an aperture array. The relation between radiation and aperture
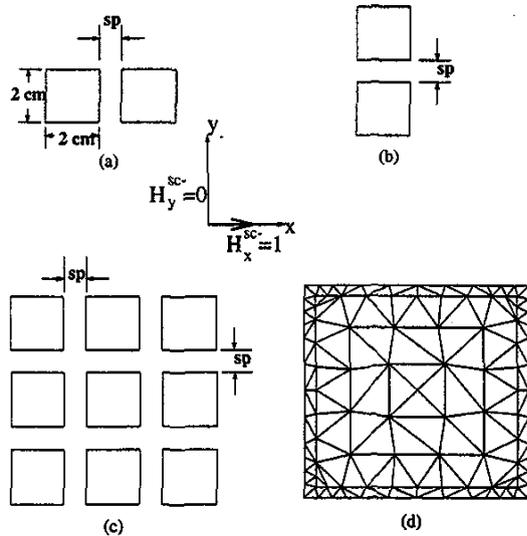
Figure 3. The aperture configurations studied: (a) Configuration 1, (b) Configuration 2, (c) Configuration 3, and, (d) mesh of one aperture used in the numerical modeling.

Figure 4. Coupling coefficient for two apertures with the incident magnetic field polarization: a) along the array axis, and b) perpendicular to the array axis.

spacing, as well as the array orientation relative to the incident wave was studied. Apertures in an infinite conducting plane and plane wave incidence were assumed. The incident magnetic field was along the x direction. Three configurations, as shown in Figure 3, were modeled. The coupling coefficient C_m for each aperture, which is indicative of the change in the EMI, is defined as

$$C_m = \frac{|\vec{M}_t^{multiple}| - |\vec{M}_t^{single}|}{|\vec{M}_t^{single}|} \tag{5}$$

where $\vec{M}_t^{multiple}$ is the magnetic current in an aperture in the presence of other apertures, and $\vec{M}_t^{single}$ is for a single aperture in a conducting plane.

The aperture size studied was 2 cm × 2 cm, and the frequency was 1 GHz. The mutual coupling coefficient for Configuration 1 (two apertures along the same direction as the incident magnetic field polarization) as a function of aperture spacing is shown in Figure 4. The mutual coupling was positive for the case of the incident magnetic field H_x polarized along the orientation of the aperture array (the x direction). The induced electric current in the conductor plane was perpendicular to the orientation of the aperture array, thus the disturbance of the current due to the introduced aperture array was maximum. The mutual coupling for Configuration 2 was negative for the case of the incident magnetic field polarization perpendicular to the orientation of aperture array. The induced electric current in the conductor plane was along the orientation of aperture array, and the disturbance of the current due
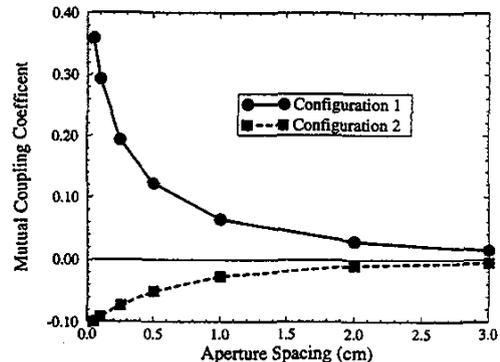
to the aperture array was less than that of Configuration 1. For the same aperture spacing, the magnitude of the mutual coupling for Configuration 1 was about three times greater than that for Configuration 2.

The fields in the apertures were also investigated to understand the mutual coupling between apertures. The calculated magnetic current densities along the y direction in the middle of the aperture for Configuration 1, and Configuration 2 are shown in Figures 5 (a) and (b), respectively. The magnetic current density $\vec{M}(\vec{r}) = \vec{E}(\vec{r}) \times \hat{z}$ is proportional to the transverse electric-field component in the apertures, and determines the field distributions for $z > 0$ [13]. The results indicate that the effect of the mutual coupling on the fields in the apertures was significant. For Configuration 1, the magnitude of the transverse electric-field component was uniformly increased with a decrease in aperture spacing. For Configuration 2, the distribution of the transverse electric-field component was relatively un-changed.

A 3 × 3 aperture array denoted as Configuration 3 in Figure 3 was also investigated. In a large array, the mutual coupling to an aperture will be mainly from the eight apertures adjacent to it. As shown in Figure 4 for two apertures, the mutual coupling from an aperture with a spacing greater than the size of the aperture was negligible. The mutual coupling as a function of aperture spacing is shown in Figure 6 for the center aperture of a 3 × 3 array. For the 2 cm × 2 cm aperture array studied herein, the mutual coupling is generally insignificant if the aperture spacing is not too small, i. e., less than 0.5 cm. For example, an aperture spacing of 1 cm yielded a mutual coupling coefficient of 0.11, which means an EMI increase of 1 dB for each aperture in the aperture array as compared to that of an independent aperture. Thus, an array of 100 apertures will generate an EMI of 100 × 1.11 × e_i (e_i is the EMI from an individual aperture), compared to the summation of EMI
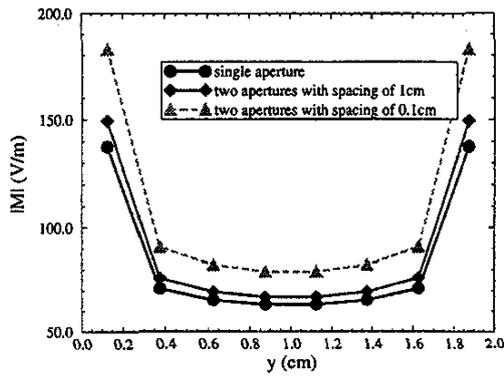
(a)
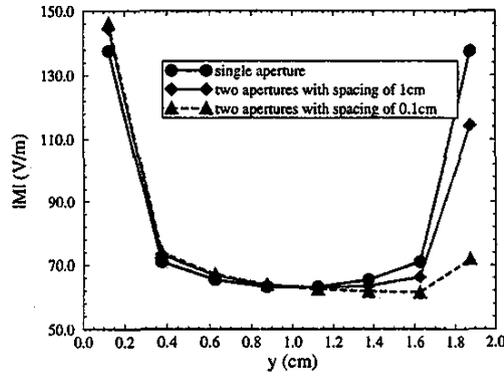
(b)

Figure 5. The magnetic current densities along the y direction in the middle of aperture for (a) Configuration 1, and (b) Configuration 2.
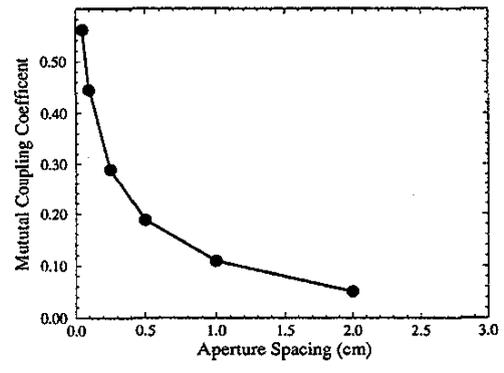

Figure 6. The mutual coupling for the aperture in the middle of a 3×3 aperture array.
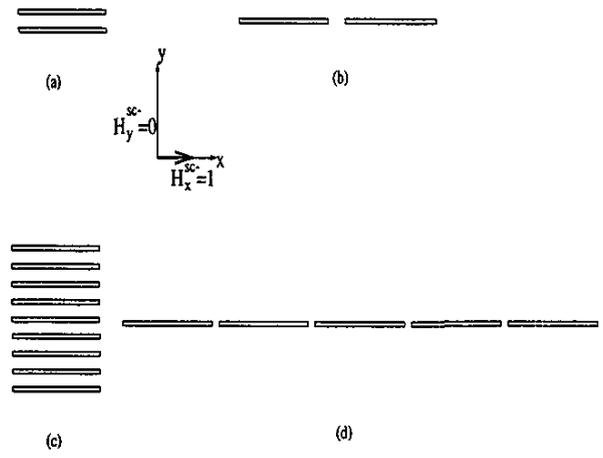

Figure 7. The slot configurations investigated: (a) two parallel slots, (b) two series slots, (c) multiple parallel slots, and, (d) multiple series slots.

from 100 individual apertures $100 \times e_i$. The difference is only 1 dB. This explains why $EMI \sim Na^3$, i. e., the N factor, generally works for square airflow aperture arrays as demonstrated in Figure 2. Arrays of circular apertures are expected to have a similar behavior.

The coupling between slots was also investigated with the same method. Configurations of series or parallel slots were studied, as shown in Figure 7. The polarization of the incident magnetic field was also along the x direction. The radiation from the slots is minimum if the incident magnetic field is polarized along the slot axis in the y direction. The slot dimensions considered were 5 $cm \times 0.1$ cm, and the frequency was 1 GHz. Two parallel or series slots were studied as a fundamental configuration for slot coupling, as shown in Figure 7 (a) and (b). The results indicate a negative coupling for parallel slots, and a positive coupling for series slots. Multiple slots were also studied to model the mutual coupling between 1-D slot arrays. Nine parallel slots were employed to obtain the mutual coupling coefficient for the slot in the middle as a typical slot in a 1-D parallel slot array, as shown in Figure 7 (c). Five series slots were employed for a 1-D series slot array as shown in Figure 7 (d), since the spacing between the slot in the middle and other slots is generally greater than that in the parallel slots. The results of mutual coupling for the multiple parallel or series slots as a function of slot spacing (edge-to-edge) are shown in Figure 8. The mutual coupling is insignificant for a slot spacing greater than 2 cm in both configurations, which is generally the case for randomly-distributed slots in shielding enclosures. The coupling between series slots is insignificant as compared to that between parallel slots, even for a spacing of 0.1 cm.
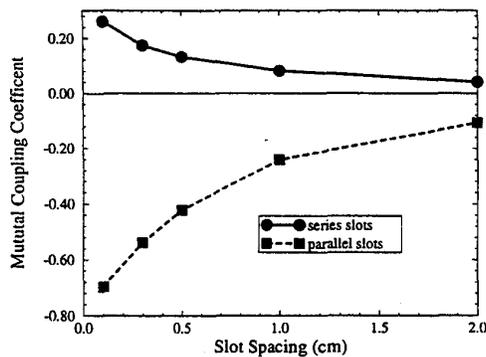
38

Figure 8. The mutual coupling coefficient for the multiple parallel or series slots.

V. Summary and Conclusion

MoM modeling was applied to investigate the mutual coupling between apertures and slots. The results indicate that the mutual coupling between apertures is generally insignificant if the spacing between apertures is not too small compared to the aperture size. This explains the EMI variation as Na^3, where N is the number of apertures, and a is the aperture size in airflow aperture arrays. The coupling between slots is also generally not important, for randomly-distributed widely-spaced slots. However, the mutual coupling between slots can be significant for arrays of parallel slots with small spacing, where the N factor may not hold.

REFERENCES

[1] H. A. Bethe, "Theory of diffraction by small holes", *Physical Review*, vol. 66, pp. 163-182, 1944.

[2] R. Mittra and S. W. Lee, *Analytical Techniques in the Theory of Guided Waves;* The Macmillon Company; New York, 1971.

[3] M. Li, S. Radu, J. L. Drewniak, T. H. Hubing, T. P. VanDoren, R. E. DuBroff, Technical Report TR98-1-029, Electromagnetic Compatibility Lab., University of Missouri-Rolla.

[4] M. Li, S. Radu, J. Nuebel, J. L. Drewniak, T. H. Hubing, T. P. VanDoren, "Design of airflow aperture arrays in shielding enclosures", *IEEE Electromagnetic Compatibility Symposium Proceedings,* pp. 1059-1063, Denver, CO, 1998.

[5] S. V. Savov, "Mutual coupling between two small circular apertures in a conducting screen", *IEEE Trans. Micro. Theory Tech.*, vol.41, pp.143-146, January 1993.

[6] A. Hessel, Y. L. Liu, J. Shmoys, "Mutual admittance between circular apertures on a large conduct-

ing sphere", *Radio Science*, vol.14, pp.35-41, January-February 1979.

[7] D. Kitchener, K. Raghavan, C. G. Parini, "Mutual coupling in a finite planar array of rectangular apertures", *Electronics Letters*, vol.23, pp.1169-1170, October 1987.

[8] A. Taflove, *Advances in Computational Electrodynamics : The Finite-Difference Time-Domain Method;* Artech House, Boston; 1998.

[9] Yuh-Sheng Tsuei, A. C. Cangellaris and J. L. Prince, "Rigorous electromagnetic modeling of chip-to-package (first-level) interconnections," *IEEE Trans. Components Hybrids Manuf. Technol.* vol. 16, pp.876-882, December 1993.

[10] J. P. Berenger, " Perfectly matched layer for the absorption of electromagnetic waves," *J. Comput. Phys.*, vol. 114, pp. 185-200, October 1994.

[11] C. M. Butler, Y. Rahmat-Samii, R. Mittra, "Electromagnetic penetration through apertures in conducting surfaces", *IEEE Trans. Antennas Propagat.*, vol. 26, pp.82-93, January 1978.

[12] S. M. Rao, D. R. Wilton, A. W. Glisson, "Electromagnetic scattering by surfaces of arbitrary shape", *IEEE Trans. Antennas Propagat.*, vol.30, pp.409-418, May 1982.

[13] C. A. Balanis, *Advanced Engineering Electromagnetics;* John Wiley & Sons; New York, 1989.